ACS OMEGA

Open Access

http://pubs.acs.org/journal/acsodf

Article

Physical Adsorption of Polyacrylic Acid on Boron Nitride Nanotube Surface and Enhanced Thermal Conductivity of Poly(vinyl alcohol) Composites

Thang Quoc Huynh, Jungwon Kim, Jeung Gon Kim,* and Seokhoon Ahn*

Cite This: *ACS Omega* 2024, 9, 31925−31932

Read Online

ACCESS | Metrics & More | Article Recommendations | Supporting Information

ABSTRACT: To fully tap into the potential of boron nitride nanotubes (BNNTs), addressing their inherent insolubility was imperative. In this study, a water-soluble polymer, poly(acrylic acid) (PAA), was employed as a surface-active reagent, using an accessible and scalable approach. The physical properties and structure of PAA-BNNT were meticulously confirmed through valuable characterization techniques, encompassing X-ray diffraction, scanning electron microscopy, Fourier-transform infrared, X-ray photoelectron spectroscopy, and thermogravimetric analysis. PAA-BNNT exhibited remarkable dispersion in water and demonstrated compatibility with the poly(vinyl alcohol) (PVA) matrix. When incorporating 30 wt % of PAA-BNNT (about 24.75 wt % net BNNT) into the PVA matrix, the thermal conductivity surged by over 21.7 times compared to pure PVA due to the uniform dispersion of high-concentration PAA-BNNT in the polymer matrix.

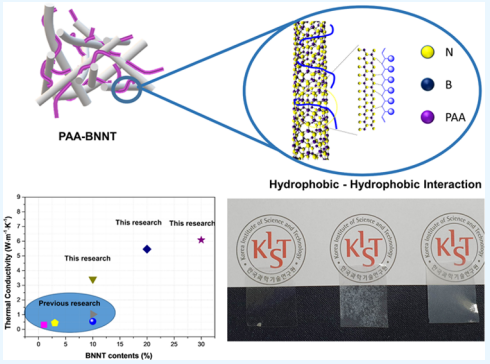

INTRODUCTION

One-dimensional (1-D) nanomaterials have garnered significant scientific attention across a wide range of disciplines due to their diverse physicochemical properties and vast potential for various applications.[1] Among these materials, boron nitride nanotubes (BNNTs) represent a unique class of 1-D structures, sharing a similar geometry to carbon nanotubes (CNTs) but with the substitution of carbon atoms by boron and nitrogen atoms in their networks.[2−6] Notably, BNNT exhibits exceptional characteristics, including high thermal stability,[7] neutron shielding,[8] superior mechanical strength,[9−15] and excellent electrical insulation properties.[16] These distinctive features make BNNT a highly promising candidate for numerous applications in fields such as nanocomposites,[17−19] thermal management,[20−22] energy harvest,[23,24] and biomedical devices.[25,26] The exploration and utilization of BNNT hold tremendous prospects for advancing scientific understanding and technological advancements in these areas.

However, the practical implementation of BNNT faces obstacles due to their tendency to form tangled bundles, primarily caused by strong van der Waals forces. As a result, BNNT is not readily dispersible in traditional organic and aqueous solvents.[27,28] To overcome this challenge, a significant breakthrough can be achieved by chemically modifying the sidewalls of BNNT to disentangle and improve their dispersibility in various solvents. Researchers have explored both covalent and noncovalent attachment strategies to address this issue. Covalent functionalization involves direct chemical reactions with stable BNNT. To enhance the stability of BNNT dispersion in solvents, diverse functional groups have been introduced. However, this approach often requires harsh conditions such as highly concentrated HNO_3, $HClO_4$ at high temperature for the initial step,[29,30] or using high energy plasma,[31] potentially damaging the outer walls of BNNT and degrading their intrinsic properties. Gas-phase surface modification techniques, such as ammonia plasma treatment and chemical vapor deposition (CVD), offer an alternative method to address some challenges while minimizing the loss of BNNT's unique properties. However, the efficiency of these methods is relatively low.[32,33] In comparison, noncovalent approaches have gained attention as they exert minimal influence on the original properties of BNNT, making them a more favorable choice in many cases. By leveraging noncovalent interactions such as $\pi-\pi$ stacking,[34−36] electrostatic interactions,[37] and hydrogen-bonding/Lewis base interaction,[38,39] the dispersibility and stability of BNNT can be enhanced without compromising their intrinsic properties. Noncovalent functionalization holds promise for various applications involving BNNT and could become the better choice in many cases.

Received: April 14, 2024
Revised: June 25, 2024
Accepted: July 1, 2024
Published: July 9, 2024

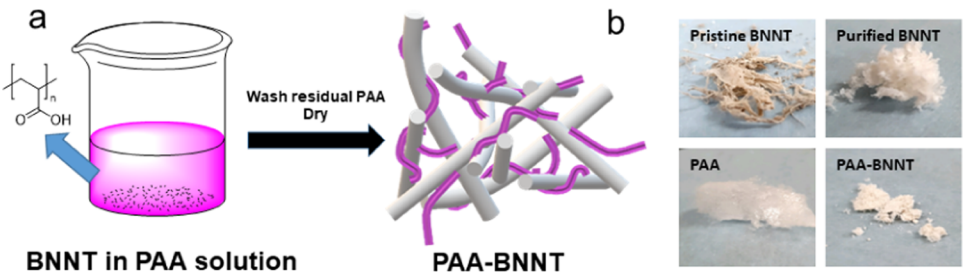

Figure 1. (a) Synthesis scheme of PAA-BNNT; (b) digital images of BNNT, PAA, and PAA-BNNT.

In this research, we perform efficient work to unbundling and functionalization via the interaction of BNNT and polyacrylic acid that was confirmed by many valuable data such as Fourier-transform infrared (FTIR) spectroscopy, X-ray diffraction (XRD), X-ray photoelectron spectroscopy (XPS), and thermogravimetric analysis (TGA). The investigation is extended by employing functionalized BNNT to fabricate well-uniform poly(vinyl alcohol) (PVA) composites with high thermal conductivity up to 21.7 times (6.08 W m^{-1} K^{-1}) in comparison to pure PVA. The effective dispersion of PAA-BNNT in the polymer system ensures the even distribution of tubes, coupled with its high density, establishing numerous contact points between tubes. This configuration fosters stable heat conduction throughout the entire film.

EXPERIMENTAL SECTION

Materials. The synthesized BNNT was provided by the High-Enthalpy Plasma Research Center at Jeonbuk National University (Republic of Korea). Poly(vinyl alcohol) (M_w 50k), 99% hydrolyzed, and polyacrylic acid (M_w 100k) 35 wt % in H_2O were purchased from Sigma-Aldrich and used without further purification.

Purification of BNNT. The synthesized BNNT was calcined in air at 650 °C for 6 h to oxidize the amorphous boron impurities. The oxidized BNNT was mixed with DI water for 1 h. The mixed suspension was precipitated for 1 h to obtain a BNNT precipitate, and a stainless metal mesh (pore size 0.045 mm) was used in the filtration process. This process was repeated to remove part of h-BN and residual boron impurities until the filtrate became transparent. The obtained BNNTs were redispersed in *tert*-butyl alcohol and freeze-dried.[40−42] Following the method presented in ref 43, the impurities were determined at 7% by FTIR, indicating that the BNNT used in this paper had a purity exceeding 90%.

PAA-BNNT Preparation. To create polymeric composites with high BNNT fractions, the process began by immersing 100 mg of BNNT in a polymer solution consisting of 1 g of PAA dissolved in 30 mL of H_2O. The BNNTs were then left for 1 day to ensure their absorption by the polymer. Subsequently, the BNNT mat underwent filtration and was washed multiple times with water to eliminate any remaining PAA. Finally, the BNNT was dried using the freeze-drying method to yield the final product.

Preparation of PVA@PAA-BNNT Nanocomposites. A defined quantity of PAA-BNNT was dispersed through 1 h of sonication. Subsequently, PVA was introduced and stirred at 70 °C until complete dissolution of the PVA was achieved. The resulting solution was then transferred into a mold. Homogeneous films were obtained after drying in air for 48 h at room temperature.

Characterization. FTIR spectroscopy was carried out using a Nicolet iS10 instrument (ThermoFisher Scientific) Infrared Spectrum Analyzer in the wavenumber range of 4000−500 cm^{-1} with KBr pellets. TGA was carried out using a TGA Q50 V20.13 Build 39 by increasing the temperature up to 700 °C (ramp: 10 °C min^{-1}) under a flowing air (90 mL min^{-1}). X-ray diffraction patterns (voltage of 40 kV, current of 30 mA) were obtained with Cu Kα radiation (λ = 0.154 nm) by Smartlab (Rigaku Corporation, Japan). The dispersion stability and dispersion degree change of the BNNTs were measured using Turbiscan Lab Expert (Formulation, France). Thermal diffusivity measurements were performed using the LaserPIT equipment (Advance Riko Inc., Japan) for the thin film in-plane measurement. The thermal diffusivity was measured two times with each sample, BNNTs 10, 20, and 30%, and the mass density (ρm) of the samples was determined using the Archimedes method.

RESULTS AND DISCUSSION

Development of BNNT Functionalization Method and Characterization. Boron nitride nanotubes are known for their dimensional properties, featuring a relatively high surface area when compared to many other materials, especially given their nanoscale dimensions. This characteristic presents the potential for weak interactions between the nanotube's surface and external (macro)molecules. Indeed, in this study, BNNT mats were immersed in the PAA solution, as depicted in Figure 1a, to facilitate their adsorption by the polymer. The formation of PAA-BNNT can be explained by PAA containing rich −COOH, known as an electron-withdrawing group, which can withdraw electrons from the carbon chain, rendering them electron-deficient sites. This results in interactions with the electron-rich N on the BNNT surface, possibly similar to mechanisms described in a certain paper.[44] The transformation of the materials used in this experiment is illustrated in Figure 1b. Each BNNT and its product exhibited variations influenced by the purification and functionalization processes. Initially, the synthesized BNNT resembled gray cotton balls due to the presence of various impurities. Following the purification process, the BNNT underwent a transformation, appearing cottony white, attributed to impurity removal and an increased BNNT content. Similarly, PAA-BNNT exhibited a white appearance like the purified BNNT, thanks to the colorless nature of PAA. Furthermore, we carefully considered the absorption of PAA, revealing that the physical absorption of PAA on the surface of BNNT could reach saturation after just 1 day. Even when the absorption process was extended to 3 days, 5 days, or longer, the weight loss, as confirmed by TGA (Figure S1), did not significantly fluctuate.

https://doi.org/10.1021/acsomega.4c03606
ACS Omega 2024, 9, 31925−31932

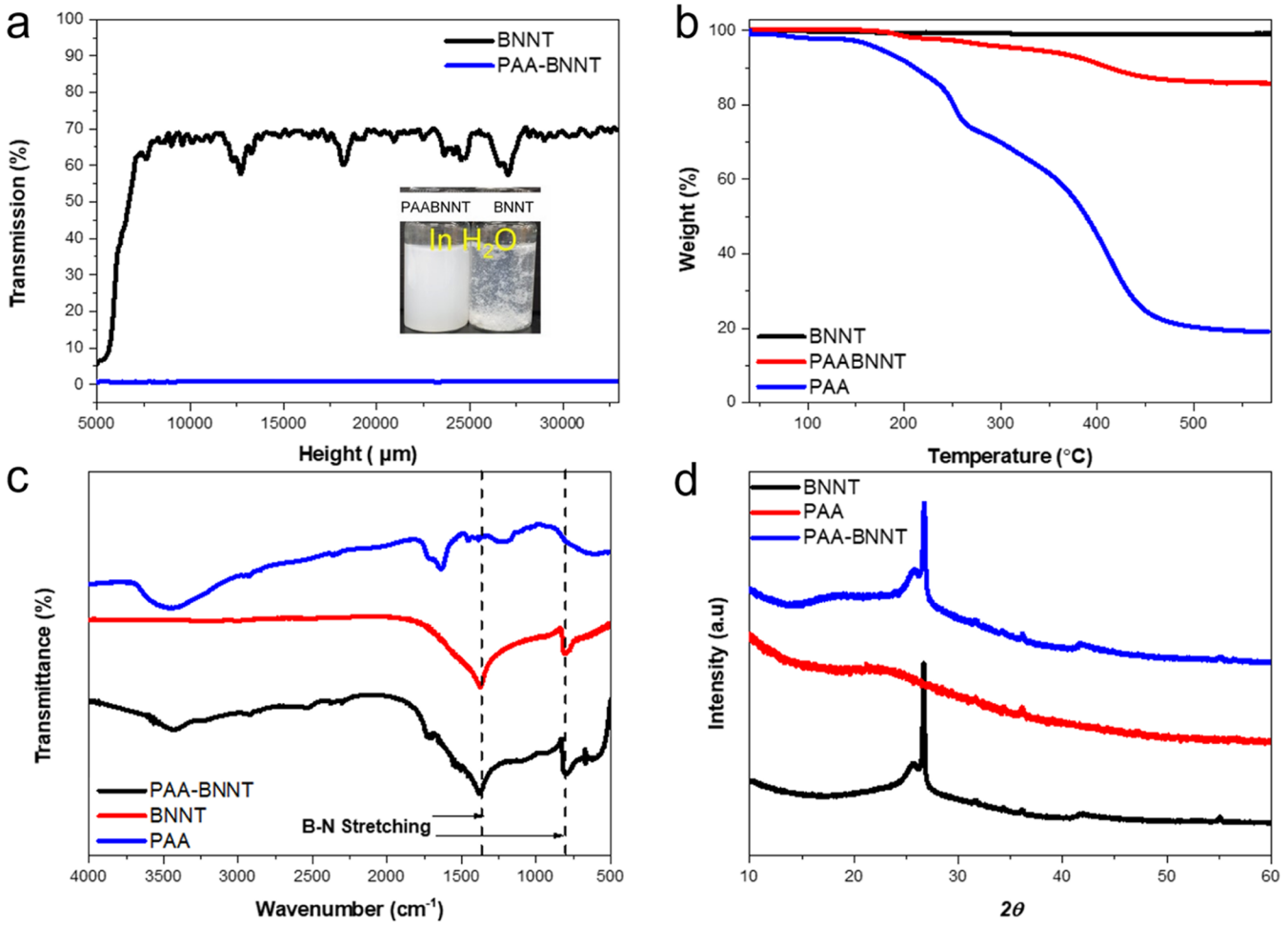

Figure 2. Comparison spectra of BNNT and PAA-BNNT. (a) Turbiscan, (b) TGA, (c) FTIR, and (d) XRD.

To deeply understand PAA-BNNT material, further characterization was conducted. Both materials (PAA-BNNT and purified BNNT, 0.4 mg/mL) were sonicated in the water for 1 h and then the samples were left at ambient temperature overnight (approximately 16 h) for stability. The dispersibility and stability of the samples were assessed using Turbiscan measurement, as illustrated in Figure 2a. The results suggest that the absorption of PAA on the surface of BNNT improved their stable dispersion. PAA-BNNT exhibited a transmission rate of approximately 1%, indicating excellent dispersibility. In contrast, this was not observed in the case of purified BNNT.

Figure 2b illustrates the TGA curves of PAA, BNNT, and PAA-BNNT. The temperature was increased from 40 to 650 °C in a nitrogen atmosphere at a heating rate of 10 °C per minute. While BNNT showed typically high stability during the whole heating process, the PAA showed almost similar stability at a lower temperature of 150 °C. However, a significant weight loss was observed at higher temperatures due to water elimination of PAA. Since 450 °C, the mass residue of PAA became constant, indicating that the cross-link has been completed, resulting in 20% of weight remaining. The PAA-BNNT showed a weight loss of about 14%, estimating the weight of the functionalized material on the thermally very stable BNNT. The net weight of PAA on BNNT can be easily figured out at around 17.5 wt %.

FTIR spectroscopy was recorded (as depicted in Figure 2c) to confirm the physical absorption of PAA on the surface of BNNT; the figure shows the spectra of PAA, BNNT, and PAA-BNNT. Spectra of PAA show three important peaks denoting 1624, 2925, and 3468 cm^{-1} that coordinated to C═O, C−H, and O−H bonds, respectively. At the same measurement conditions, spectra of the BNNT show asymmetric B−N with 1375 and 796 cm^{-1} B−N stretching and B−N−B expansion. Consequently, PAA-BNNT exhibits all characteristics of peak, combining both PAA and purified BNNT.

The diffractogram of the PAA polymer was observed and is depicted in Figure 2d, which shows a low intense and broad signal at around the angle of $2\theta = 21°$,[45] demonstrating the low crystalline nature of the polymer. Purified BNNT contains crystalline impurities, including h-BN, which is characterized by a distinct peak at 26.7° in the XRD analysis. On the other hand, noncrystalline BNNT exhibits a broader peak at 25.8°. Notably, all amorphous boron peaks in the XRD graph disappeared after the purification process. These observations confirm the consistency of the XRD patterns with prior studies. The XRD pattern of PAA-BNNT closely resembles that of purified BNNT, indicating that PAA functionalization is an effective method that preserves the properties of BNNT while efficiently removing amorphous boron and h-BN, all without requiring a separate purification step.

The XPS technique was utilized to analyze the element content, and the results confirmed that noncovalent functionalization of PAA had successfully formed a stable bond on the surface of BNNT. In the C 1s spectrum depicted in Figure 3b,

https://doi.org/10.1021/acsomega.4c03606
ACS Omega 2024, 9, 31925−31932

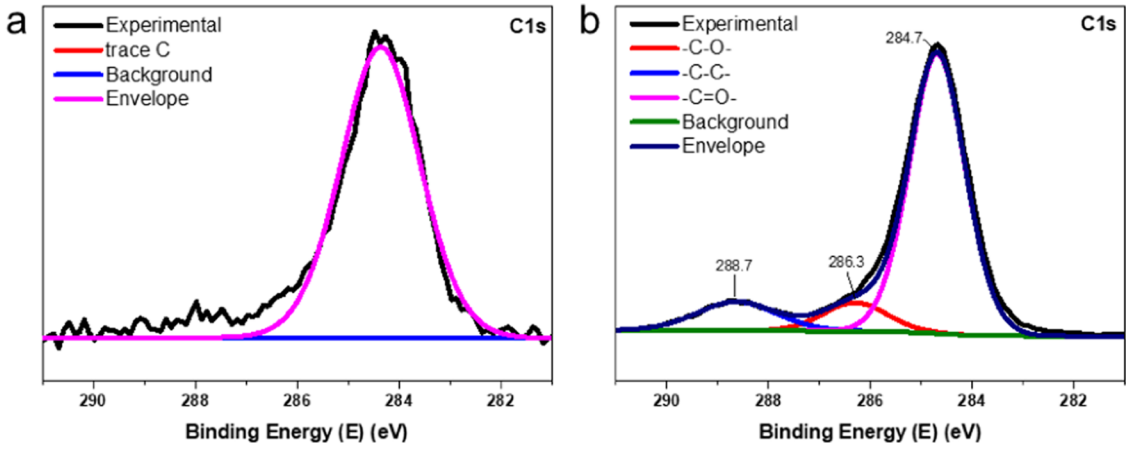

Figure 3. C 1s XPS spectrum of (a) pristine BNNT and (b) PAA-BNNT.

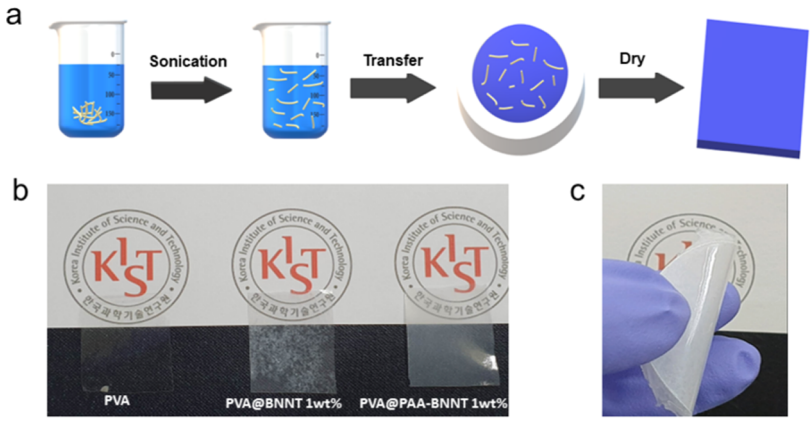

Figure 4. (a) Fabrication scheme of PVA@PAA-BNNT; (b) digital image of PVA, PVA@BNNT, and PVA@PAA-BNNT at 1 wt %; and (c) PVA@PAA-BNNT at 30 wt %.

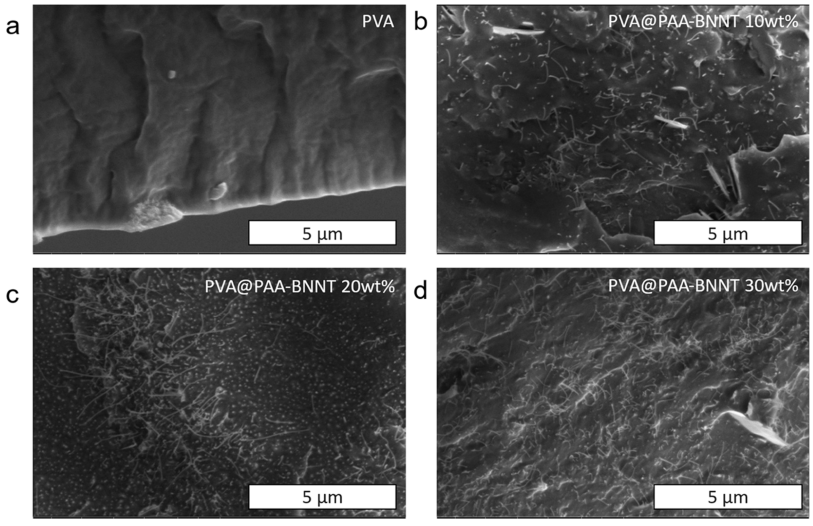

Figure 5. SEM cross-sectional images of the PAA-BNNT/PVA composite films: (a) pure PVA, (b) 10 wt % PAA-BNNT, (c) 20 wt % PAA-BNNT, and (d) 30 wt % PAA-BNNT.

distinct peaks were observed for various carbon species, including C−C at 284.7 eV, C−O at 286.3 eV, and C═O at 288.7 eV, indicating the presence of PAA polymers on the BNNT's surface. In contrast, the C 1s spectrum of the pristine BNNT (Figure 3a) displayed only a minimal or trace signal, emphasizing the effectiveness of the noncovalent functionalization process in introducing carbon chains onto the BNNT's surface.

Enhancement of Thermal Conductivity of PVA@PAA-BNNT Nanocomposites. To create composites that contain evenly dispersed BNNT, it is essential to ensure the consistent distribution of BNNT within the processing solvent. This

https://doi.org/10.1021/acsomega.4c03606
ACS Omega 2024, 9, 31925−31932

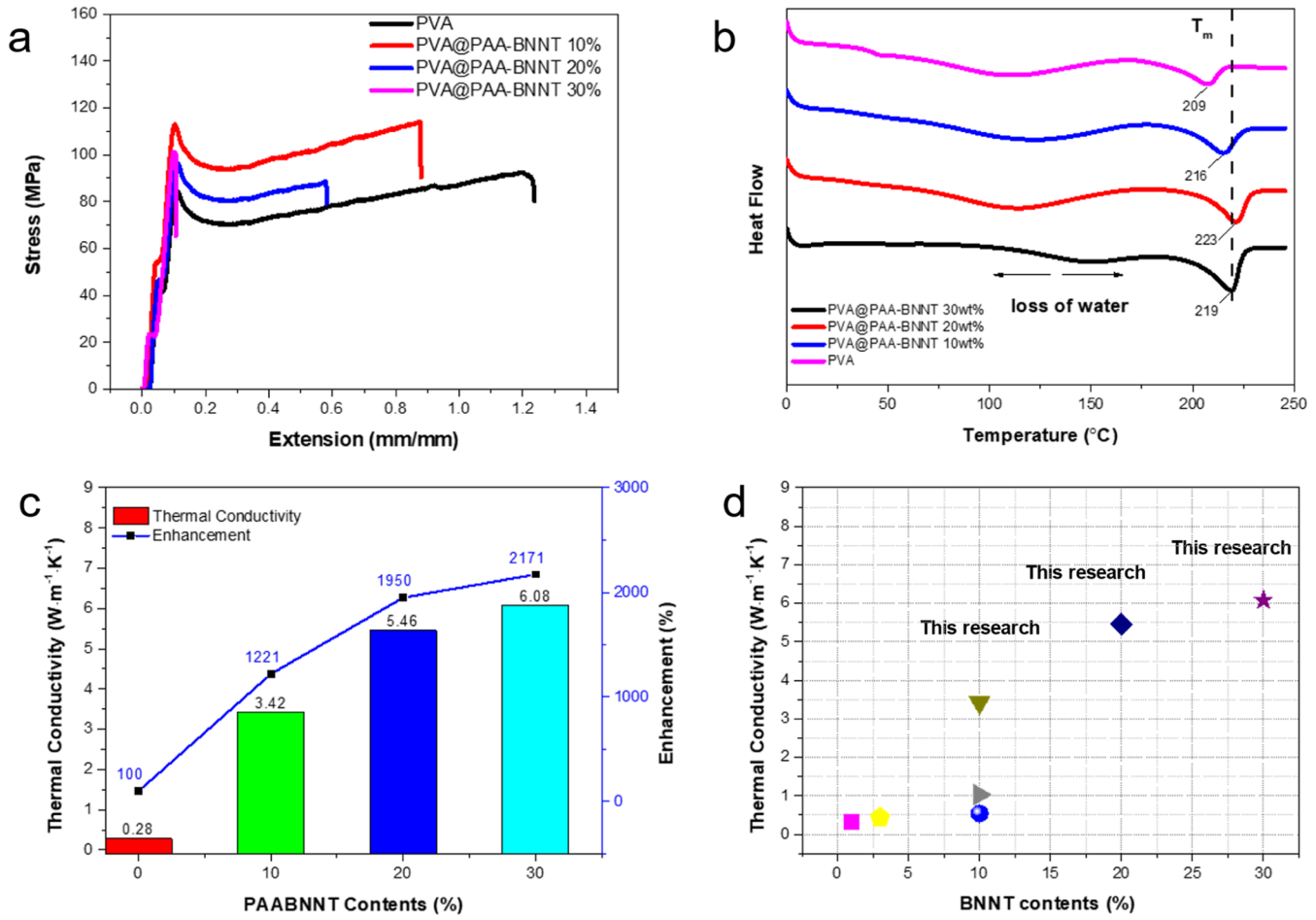

Figure 6. (a) Stress−strain curves of the pure PVA film and PVA@PAA-BNNT; (b) DSC profile of samples; (c) thermal conductivity and enhancement of PVA@PAA-BNNT; and (d) comparison with prior study.

uniform dispersion should be maintained even after adding the polymer into the solution and continue until the solvent completely evaporates.[46] Indeed, the stability of the PAA-BNNT solution led to the facile preparation of the PVA@PAA-BNNT nanocomposite film through the solvent casting method by loading 10−30 wt % of PAA-BNNT based on the weight of PVA. The procedure is demonstrated in Figure 4a.

As can be seen in Figure 4b, pure BNNT exhibits an unstable dispersion and tends to agglomerate within the PVA matrix, resulting in a nonuniform composite. In contrast, the PVA@PAA-BNNT composite demonstrates an exceptionally uniform dispersion of nanotubes within the PVA matrix. Moreover, composites containing up to 30 wt % (as depicted in Figure 4c) of PAA-BNNT can be easily folded, providing durability and flexibility to the BNNT. However, when the PAA-BNNT content exceeds 30 wt %, agglomeration initiates within the PVA matrix, likely attributed to stronger interactions among the nanotubes than between the nanotubes and the polymer matrix. Previous research established the potential for strong hydrogen bond formation between PVA and PAA.[47,48] These intermolecular interactions including PAA−PVA and PAA-BNNT could significantly enhance the properties of PVA@PAA-BNNT, leading to the creation of a stronger composite.

The morphologies of the composites were also characterized with cross-sectional SEM images as shown in Figure 5. In all samples, Figure 5a−d, the added PAA-BNNT inside the PVA matrix was identified as bright dots and tubes representing the cutting faces of the BNNT stems and multiple BNNT. PVA (Figure 5a) shows no signal of BNNT used as a comparison sample. In addition, for the PAA-BNNT containing samples, Figure 5b−d, the BNNT was generally well-distributed within the PVA matrix, and some of the BNNTs randomly arranged in the horizontal and vertical directions were also observed in the SEM cross-sectional images. Especially, the 30 wt % BNNT sample exhibited a denser distribution of BNNTs compared to the 10 and 20 wt % samples. It is worth noting that the excessive addition of BNNT to PVA can result in the mechanical degradation of PVA composites due to the formation of micropores and/or grained PVA matrix near regions with excessively dense BNNT.

The mechanical properties of the composite were investigated through a tensile test (Figure 6a). The incorporation of PAA-BNNT additives significantly reduced the elongation property of the PVA films. While the pure PVA film exhibited an extension rate of 120%, the addition of 10, 20, and 30% of PAA-BNNT resulted in decreased rates of 86, 58, and 10%, respectively. Additionally, studies have shown that incorporating various reinforcing materials into the matrix can enhance the strength properties of composites.[6,49,50] Indeed, this study witnessed the stress values that increased from 84 to 112, 96, and 100 MPa, respectively.

https://doi.org/10.1021/acsomega.4c03606
ACS Omega 2024, 9, 31925−31932

The DSC profiles of PVA and its composites are illustrated in Figure 6b. The broad peak observed in the temperature range from approximately 60−170 °C was attributed to the release of water, a common occurrence in PVA-based composites.[50] Subsequently, the melting point of the PVA (Tm) and its composite followed, indicated by a small, relatively sharp peak ranging from 209 to 223 °C. This observation suggests structural stabilization of composites up to around 200 °C, thereby partially revealing the maximum working temperature of the composites.

It has been reported that incorporating 10 wt % or more of BNNT is unfavorable due to issues related to dispersion and detrimental effects on the mechanical properties of the base materials.[51−53] However, as the weight percentage of PAA-BNNT increases, there is a noticeable improvement in thermal conductivity (as depicted in Figure 6c). For instance, at 10 wt %, the thermal conductivity was approximately 12 times that of a PVA film (0.28 W m^{-1} K^{-1}).[54] When 20 wt % of PAA-BNNT was added to the PVA matrix, there was a significant enhancement in thermal conductivity, reaching an increase of nearly 19.5 times. Notably, a remarkable 21.7-fold enhancement in thermal conductivity was observed when comparing pure PVA to a sample containing 30 wt % of PAA-BNNT. This particular sample exhibited the highest thermal conductivity, measuring at 6.08 W m^{-1} K^{-1}. Figure 6d illustrates a comparison with previous studies regarding PVA@BNNT composites, highlighting that our composites excel not only in their high BNNT content but also in terms of superior thermal conductivity performance.[55−58] A thermal conductivity of 3.4 W m^{-1} K^{-1} at 10 wt % in the present case is much higher than the referenced result (∼1 W m^{-1} K^{-1}).[57] In the reference case, PVA and BNNT were physically mixed in the solvent without using a dispersant, which led to BNNT aggregating in the matrix. However, in the present case, the dispersant helps the BNNT to be well-dispersed in the PVA matrix, as shown in Figures 2 and 4. Additionally, the thermal conductivity for the present case was measured along the film surface using LaserPIT equipment. These facts could account for the higher thermal conductivity observed compared to the reference results.

CONCLUSIONS

BNNT was functionalized and unbundled by PAA using an environmentally friendly, easy-to-scale method, which significantly enhanced their dispersibility in water. The physical properties and structure of PAA-BNNT were carefully confirmed through valuable characterization techniques such as XRD, FTIR, XPS, and TGA. Furthermore, it was observed that PAA-BNNT can be excellently integrated into a PVA matrix, resulting in a synergistic enhancement of thermal conductivity. When a 30 wt % PAA-BNNT load was used, the thermal conductivity of the PVA composite reached 6.08 W m^{-1} K^{-1}, which is more than 21.7 times higher than that of pure PVA. This outstanding property opens wide-ranging potential for the fabrication of nanocomposites with diverse applications.

ASSOCIATED CONTENT

Supporting Information

The Supporting Information is available free of charge at https://pubs.acs.org/doi/10.1021/acsomega.4c03606.

Data includes an investigation of BNNT absorption over time; SEM of BNNT and PAA-BNNT; full XPS data set; thermal conductivity; and related information on the PVA@PAA-BNNT composite (PDF)

AUTHOR INFORMATION

Corresponding Authors

Jeung Gon Kim − *Department of Chemistry and Research, Institute of Physics and Chemistry, Jeonbuk National University, Jeonju 54896 Jeonbuk-do, Republic of Korea; Department of JBNU-KIST Industry-Academia Convergence Research, Jeonbuk National University, Jeonju 54896 Jeonbuk-do, Republic of Korea;* orcid.org/0000-0003-1685-2833; Email: jeunggonkim@jbnu.ac.kr

Seokhoon Ahn − *Institute of Advanced Composite Materials, Korea Institute of Science and Technology (KIST), Wanju-gun 55324 Jeonbuk-do, Republic of Korea; Department of JBNU-KIST Industry-Academia Convergence Research, Jeonbuk National University, Jeonju 54896 Jeonbuk-do, Republic of Korea;* orcid.org/0000-0002-3960-3197; Email: ahn75@kist.re.kr

Authors

Thang Quoc Huynh − *Institute of Advanced Composite Materials, Korea Institute of Science and Technology (KIST), Wanju-gun 55324 Jeonbuk-do, Republic of Korea; Department of Chemistry and Research, Institute of Physics and Chemistry, Jeonbuk National University, Jeonju 54896 Jeonbuk-do, Republic of Korea;* orcid.org/0000-0001-5102-8140

Jungwon Kim − *Institute of Advanced Composite Materials, Korea Institute of Science and Technology (KIST), Wanju-gun 55324 Jeonbuk-do, Republic of Korea*

Complete contact information is available at: https://pubs.acs.org/10.1021/acsomega.4c03606

Author Contributions

T.Q.H.: conceptualization, validation, investigation, and writing—original draft; J.W.K.: investigation; and J.G.K. and A.S.H: supervision and writing—review and editing. The manuscript was written through contributions of all authors. All authors have given approval to the final version of the manuscript.

Notes

The authors declare no competing financial interest.

ACKNOWLEDGMENTS

This work was supported by the Commercialization Promotion Agency for R&D Outcomes (COMPA) grant (RS-2023-00304729) funded by the Korean Government (Ministry of Science and ICT, 2023) and the Korea Institute of Science and Technology (KIST) Institutional Program (2E33323).

ABBREVIATIONS

BNNT - boron nitride nanotube; SEM - scanning electron microscope; XPS - X-ray photoelectron spectroscopy; FTIR - Fourier-transform infrared spectroscopy; XRD - X-ray diffraction; and TGA - thermogravimetric analysis

REFERENCES

(1) Xia, Y.; Yang, P.; Sun, Y.; Wu, Y.; Mayers, B.; Gates, B.; Yin, Y.; Kim, F.; Yan, H. One-Dimensional Nanostructures: Synthesis,

Characterization, and Applications. *Adv. Mater.* **2003**, *15* (5), 353−389.
(2) Maselugbo, A. O.; Harrison, H. B.; Alston, J. R. Boron Nitride Nanotubes: A Review of Recent Progress on Purification Methods and Techniques. *J. Mater. Res.* **2022**, *37* (24), 4438−4458.
(3) Smith, K. K.; Redeker, N. D.; Rios, J. C.; Mecklenburg, M. H.; Marcischak, J. C.; Guenthner, A. J.; Ghiassi, K. B. Surface Modification and Functionalization of Boron Nitride Nanotubes via Condensation with Saturated and Unsaturated Alcohols for High Performance Polymer Composites. *ACS Appl. Nano Mater.* **2019**, *2* (7), 4053−4060.
(4) Gao, Z.; Fujioka, K.; Sawada, T.; Zhi, C.; Bando, Y.; Golberg, D.; Aizawa, M.; Serizawa, T. Noncovalent Functionalization of Boron Nitride Nanotubes Using Water-Soluble Synthetic Polymers and the Subsequent Preparation of Superhydrophobic Surfaces. *Polym. J.* **2013**, *45* (5), 567−570.
(5) Jin, J.-U.; Jang, S. G.; Ahn, S.; Kim, D.-Y.; Hahn, J. R.; You, N.-H. Noncovalently Functionalized Boron Nitride Nanotubes and Polymer Nanocomposites with Water-Soluble Poly (Amic Acid) Salt. *Appl. Surf. Sci.* **2023**, *623*, No. 157082.
(6) Lee, S.; Jeon, I. S.; Jho, J. Y. Mechanical Properties of Polyetheretherketone Composites with Surface-Modified Hydroxyapatite Nanofibers and Carbon Fibers. *Macromol. Res.* **2022**, *30* (4), 261−270.
(7) Chen, X.; Dmuchowski, C. M.; Park, C.; Fay, C. C.; Ke, C. Quantitative Characterization of Structural and Mechanical Properties of Boron Nitride Nanotubes in High Temperature Environments. *Sci. Rep.* **2017**, *7* (1), 11388.
(8) Thibeault, S. A.; Kang, J. H.; Sauti, G.; Park, C.; Fay, C. C.; King, G. C. Nanomaterials for Radiation Shielding. *MRS Bull.* **2015**, *40* (10), 836−841.
(9) Wei, X.; Wang, M.-S.; Bando, Y.; Golberg, D. Tensile Tests on Individual Multi-Walled Boron Nitride Nanotubes. *Adv. Mater.* **2010**, *22* (43), 4895−4899.
(10) Chopra, N. G.; Zettl, A. Measurement of the Elastic Modulus of a Multi-Wall Boron Nitride Nanotube. *Solid State Commun.* **1998**, *105* (5), 297−300.
(11) Arenal, R.; Wang, M.-S.; Xu, Z.; Loiseau, A.; Golberg, D. Young Modulus, Mechanical and Electrical Properties of Isolated Individual and Bundled Single-Walled Boron Nitride Nanotubes. *Nanotechnology* **2011**, *22* (26), No. 265704.
(12) Hernández, E.; Goze, C.; Bernier, P.; Rubio, A. Elastic properties of C and B x C y N z composite nanotubes. *Phys. Rev. Lett.* **1998**, *80* (20), 4502 DOI: 10.1103/PhysRevLett.80.4502.
(13) Ghassemi, H. M.; Lee, C. H.; Yap, Y. K.; Yassar, R. S. Real-Time Fracture Detection of Individual Boron Nitride Nanotubes in Severe Cyclic Deformation Processes. *J. Appl. Phys.* **2010**, *108* (2), No. 024314.
(14) Tang, D.-M.; Ren, C.-L.; Wei, X.; Wang, M.-S.; Liu, C.; Bando, Y.; Golberg, D. Mechanical Properties of Bamboo-like Boron Nitride Nanotubes by In Situ TEM and MD Simulations: Strengthening Effect of Interlocked Joint Interfaces. *ACS Nano* **2011**, *5* (9), 7362−7368.
(15) Suryavanshi, A. P.; Yu, M.-F.; Wen, J.; Tang, C.; Bando, Y. Elastic Modulus and Resonance Behavior of Boron Nitride Nanotubes. *Appl. Phys. Lett.* **2004**, *84* (14), 2527−2529.
(16) Kim, J. H.; Pham, T. V.; Hwang, J. H.; Kim, C. S.; Kim, M. J. Boron Nitride Nanotubes: Synthesis and Applications. *Nano Convergence* **2018**, *5* (1), 17.
(17) Shim, J.; Son, D. I.; Lee, J. S.; Lee, J.; Lim, G.-H.; Cho, H.; Kim, E.; Bu, S. D.; Im, S.; Jeong, C. K.; Rezvani, S.; Park, S. S.; Park, Y. J. BNNT-ZnO QDs Nanocomposites for Improving Piezoelectric Nanogenerator and Piezoelectric Properties of Boron Nitride Nanotube. *Nano Energy* **2022**, *93*, No. 106886.
(18) Zeng, X.; Sun, J.; Yao, Y.; Sun, R.; Xu, J.-B.; Wong, C.-P. A Combination of Boron Nitride Nanotubes and Cellulose Nanofibers for the Preparation of a Nanocomposite with High Thermal Conductivity. *ACS Nano* **2017**, *11* (5), 5167−5178.
(19) Martinez-Rubi, Y.; Ashrafi, B.; Jakubinek, M. B.; Zou, S.; Kim, K. S.; Cho, H.; Simard, B. Nanocomposite Fabrics with High Content of Boron Nitride Nanotubes for Tough and Multifunctional Composites. *J. Mater. Res.* **2022**, *37* (24), 4553−4565.
(20) Wagner, K.; Paquet, C.; Martinez-Rubi, Y.; Genest, M.; Guan, J.; Sampson, K. L.; Kim, K. S.; Kell, A. J.; Malenfant, P. R. L.; Lessard, B. H. Boron Nitride Nanotube Coatings for Thermal Management of Printed Silver Inks on Temperature Sensitive Substrates. *Adv. Electron. Mater.* **2021**, *7* (5), No. 2001035.
(21) Du, P.-Y.; Wang, Z.-X.; Ren, J.-W.; Zhao, L.-H.; Jia, S.-L.; Jia, L.-C. Scalable Polymer-Infiltrated Boron Nitride Nanoplatelet Films with High Thermal Conductivity and Electrical Insulation for Thermal Management. *ACS Appl. Electron. Mater.* **2022**, *4* (9), 4622−4631.
(22) Huff, C. F.; News, N.; Jordan, K. C.; News, N.; Stevens, J. C. Henneberg, Newport News, VA (US).
(23) Zhang, D.; Yapici, N.; Oakley, R.; Yap, Y. K. The Rise of Boron Nitride Nanotubes for Applications in Energy Harvesting, Nanoelectronics, Quantum Materials, and Biomedicine. *J. Mater. Res.* **2022**, *37* (24), 4605−4619.
(24) Kang, S. H.; Choi, G. M.; Rahmannezhad, J.; Kim, C.; Kim, Y.-K.; Ahn, S.; Jang, S. G.; Kim, M. J.; Lee, H. S. Purity and Concentration Dependence of Piezoelectricity and Thermal Conductivity of Boron Nitride Nanotubes. *J. Mater. Res.* **2022**, *37* (24), 4544−4552.
(25) Ciofani, G.; Raffa, V.; Menciassi, A.; Cuschieri, A. Boron Nitride Nanotubes: An Innovative Tool for Nanomedicine. *Nano Today* **2009**, *4* (1), 8−10.
(26) Ozcan, F.; Cagil, E. M. Preparation of Hexagonal Boron Nitride Polymer Systems with One-Step Sol−Gel Synthesis for pH-Controlled Drug Delivery. *Macromol. Res.* **2024**, *32*, 337.
(27) Chang, M. S.; Jang, M.-S.; Yang, S.; Yu, J.; Kim, T.; Kim, S.; Jeong, H.; Park, C. R.; Jeong, J. W. Electrostabilized Homogeneous Dispersion of Boron Nitride Nanotubes in Wide-Range of Solvents Achieved by Surface Polarity Modulation through Pyridine Attachment. *Nano Res.* **2020**, *13* (2), 344−352.
(28) Golberg, D.; Bando, Y.; Tang, C. C.; Zhi, C. Y. Boron Nitride Nanotubes. *Adv. Mater.* **2007**, *19* (18), 2413−2432.
(29) Smith, K. K.; Redeker, N. D.; Rios, J. C.; Mecklenburg, M. H.; Marcischak, J. C.; Guenthner, A. J.; Ghiassi, K. B. Surface Modification and Functionalization of Boron Nitride Nanotubes via Condensation with Saturated and Unsaturated Alcohols for High Performance Polymer Composites. *ACS Appl. Nano Mater.* **2019**, *2* (7), 4053−4060.
(30) Ciofani, G.; Genchi, G. G.; Liakos, I.; Athanassiou, A.; Dinucci, D.; Chiellini, F.; Mattoli, V. A Simple Approach to Covalent Functionalization of Boron Nitride Nanotubes. *J. Colloid Interface Sci.* **2012**, *374* (1), 308−314.
(31) Iannitto, R.; Shin, H.; Martinez Rubi, Y.; Simard, B.; Coulombe, S. In-Flight Plasma Functionalization of Boron Nitride Nanotubes with Ammonia for Composite Applications. *ACS Appl. Nano Mater.* **2020**, *3* (1), 294−302.
(32) Torres-Castillo, C. S.; Tavares, J. R. Covalent Functionalization of Boron Nitride Nanotubes through Photo-Initiated Chemical Vapour Deposition. *Can. J. Chem. Eng.* **2023**, *101* (3), 1410−1420.
(33) Iannitto, R.; Shin, H.; Martinez Rubi, Y.; Simard, B.; Coulombe, S. In-Flight Plasma Functionalization of Boron Nitride Nanotubes with Ammonia for Composite Applications. *ACS Appl. Nano Mater.* **2020**, *3* (1), 294−302.
(34) Velayudham, S.; Lee, C. H.; Xie, M.; Blair, D.; Bauman, N.; Yap, Y. K.; Green, S. A.; Liu, H. Noncovalent Functionalization of Boron Nitride Nanotubes with Poly(p-Phenylene-Ethynylene)s and Polythiophene. *ACS Appl. Mater. Interfaces* **2010**, *2* (1), 104−110, DOI: 10.1021/am900613j.
(35) Zhi, C.; Bando, Y.; Wang, W.; Tang, C.; Kuwahara, H.; Golberg, D. DNA-Mediated Assembly of Boron Nitride Nanotubes. *Chem. - Asian J.* **2007**, *2* (12), 1581−1585, DOI: 10.1002/asia.200700246.

https://doi.org/10.1021/acsomega.4c03606
ACS Omega 2024, 9, 31925−31932

(36) Zhi, C.; Bando, Y.; Tang, C.; Xie, R.; Sekiguchi, T.; Golberg, D. Perfectly Dissolved Boron Nitride Nanotubes Due to Polymer Wrapping. *J. Am. Chem. Soc.* **2005**, *127* (46), 15996−15997.
(37) Chang, M. S.; Jang, M.-S.; Yang, S.; Yu, J.; Kim, T.; Kim, S.; Jeong, H.; Park, C. R.; Jeong, J. W. Electrostabilized Homogeneous Dispersion of Boron Nitride Nanotubes in Wide-Range of Solvents Achieved by Surface Polarity Modulation through Pyridine Attachment. *Nano Res.* **2020**, *13* (2), 344−352.
(38) Lee, S.-H.; Kang, M.; Lim, H.; Moon, S. Y.; Kim, M. J.; Jang, S. G.; Lee, H. J.; Cho, H.; Ahn, S. Purification of Boron Nitride Nanotubes by Functionalization and Removal of Poly(4-Vinylpyridine). *Appl. Surf. Sci.* **2021**, *555*, No. 149722.
(39) Shin, H.; Yeverovich, E.; Kim, K. S. Poly(4-Vinylpyridine) Adsorption on Boron Nitride Nanotubes and Hexagonal Boron Nitride: A Comparative Molecular Dynamics Study. *J. Mater. Res.* **2022**, *37* (24), 4483−4495.
(40) Lee, S.-H.; Kim, M. J.; Ahn, S.; Koh, B. Purification of Boron Nitride Nanotubes Enhances Biological Application Properties. *Int. J. Mol. Sci.* **2020**, *21* (4), 1529.
(41) Ko, J.; Kim, H. M.; Moon, S. Y.; Ahn, S.; Im, S. G.; Joo, Y. Highly Pure, Length-Sorted Boron Nitride Nanotubes by Gel Column Chromatography. *Chem. Mater.* **2021**, *33* (12), 4723−4732.
(42) Ko, J.; Kim, D.; Sim, G.; Moon, S. Y.; Lee, S. S.; Jang, S. G.; Ahn, S.; Im, S. G.; Joo, Y. Scalable, Highly Pure, and Diameter-Sorted Boron Nitride Nanotube by Aqueous Polymer Two-Phase Extraction. *Small Methods* **2023**, *7* (4), No. 2201341.
(43) Harrison, H.; Lamb, J. T.; Nowlin, K. S.; Guenthner, A. J.; Ghiassi, K. B.; Kelkar, A. D.; Alston, J. R. Quantification of Hexagonal Boron Nitride Impurities in Boron Nitride Nanotubes via FTIR Spectroscopy. *Nanoscale Adv.* **2019**, *1* (5), 1693−1701.
(44) Zeng, X.; Sun, J.; Yao, Y.; Sun, R.; Xu, J.-B.; Wong, C.-P. A Combination of Boron Nitride Nanotubes and Cellulose Nanofibers for the Preparation of a Nanocomposite with High Thermal Conductivity. *ACS Nano* **2017**, *11* (5), 5167−5178.
(45) Swain, S. K.; Prusty, K. Biomedical Applications of Acrylic-Based Nanohydrogels. *J. Mater. Sci.* **2018**, *53* (4), 2303−2325.
(46) Chang, M. S.; Jang, M.-S.; Yang, S.; Yu, J.; Kim, T.; Kim, S.; Jeong, H.; Park, C. R.; Jeong, J. W. Electrostabilized Homogeneous Dispersion of Boron Nitride Nanotubes in Wide-Range of Solvents Achieved by Surface Polarity Modulation through Pyridine Attachment. *Nano Res.* **2020**, *13* (2), 344−352.
(47) Liu, T.; Jiao, C.; Peng, X.; Chen, Y.-N.; Chen, Y.; He, C.; Liu, R.; Wang, H. Super-Strong and Tough Poly(Vinyl Alcohol)/Poly(Acrylic Acid) Hydrogels Reinforced by Hydrogen Bonding. *J. Mater. Chem. B* **2018**, *6* (48), 8105−8114.
(48) Molisso, A.; Mangiapia, G.; D'Errico, G.; Sartorio, R. Interaction of Poly(Vinyl Alcohol) with Poly(Acrylic Acid) and with Sodium Polyacrylate in Aqueous Solutions: A Volumetric Study at 25 °C. *J. Solution Chem.* **2010**, *39* (11), 1627−1635.
(49) Wu, Y.; Xue, Y.; Qin, S.; Liu, D.; Wang, X.; Hu, X.; Li, J.; Wang, X.; Bando, Y.; Golberg, D.; Chen, Y.; Gogotsi, Y.; Lei, W. BN Nanosheet/Polymer Films with Highly Anisotropic Thermal Conductivity for Thermal Management Applications. *ACS Appl. Mater. Interfaces* **2017**, *9* (49), 43163−43170.
(50) Remiš, T.; Bělský, P.; Kovářík, T.; Kadlec, J.; Ghafouri Azar, M.; Medlín, R.; Vavruňková, V.; Deshmukh, K.; Sadasivuni, K. K. Study on Structure, Thermal Behavior, and Viscoelastic Properties of Nanodiamond-Reinforced Poly (Vinyl Alcohol) Nanocomposites. *Polymers* **2021**, *13* (9), 1426.
(51) Zhi, C. Y.; Bando, Y.; Wang, W. L.; Tang, C. C.; Kuwahara, H.; Golberg, D. Mechanical and Thermal Properties of Polymethyl Methacrylate-BN Nanotube Composites. *J. Nanomater.* **2008**, *2008*, No. e642036.
(52) Zhi, C.; Bando, Y.; Tang, C.; Honda, S.; Kuwahara, H.; Golberg, D. Boron Nitride Nanotubes/Polystyrene Composites. *J. Mater. Res.* **2006**, *21* (11), 2794−2800.
(53) Yoo, H. I.; Moon, S. Y. Thermal Transfer Improvement in Polyvinyl Alcohol Films by Mixing with Boron Nitride Nanotubes Synthesized Using a Radio-Frequency Inductively Coupled Thermal Plasma. *Curr. Appl. Phys.* **2023**, *54*, 10−15.
(54) Wu, Y.; Ye, K.; Liu, Z.; Wang, M.; Chee, K. W. A.; Lin, C.-T.; Jiang, N.; Yu, J. Effective Thermal Transport Highway Construction within Dielectric Polymer Composites via a Vacuum-Assisted Infiltration Method. *J. Mater. Chem. C* **2018**, *6* (24), 6494−6501.
(55) Terao, T.; Bando, Y.; Mitome, M.; Zhi, C.; Tang, C.; Golberg, D. Thermal Conductivity Improvement of Polymer Films by Catechin-Modified Boron Nitride Nanotubes. *J. Phys. Chem. C* **2009**, *113* (31), 13605−13609.
(56) Lu, X.; Nautiyal, P.; Bustillos, J.; Loganathan, A.; Zhang, C.; Chen, Y.; Boesl, B.; Agarwal, A. Hydroxylated Boron Nitride Nanotube-Reinforced Polyvinyl Alcohol Nanocomposite Films with Simultaneous Improvement of Mechanical and Thermal Properties. *Polym. Compos.* **2020**, *41* (12), 5182−5194.
(57) Yoo, H. I.; Moon, S. Y. Thermal Transfer Improvement in Polyvinyl Alcohol Films by Mixing with Boron Nitride Nanotubes Synthesized Using a Radio-Frequency Inductively Coupled Thermal Plasma. *Curr. Appl. Phys.* **2023**, *54*, 10−15.
(58) Terao, T.; Zhi, C.; Bando, Y.; Mitome, M.; Tang, C.; Golberg, D. Alignment of Boron Nitride Nanotubes in Polymeric Composite Films for Thermal Conductivity Improvement. *J. Phys. Chem. C* **2010**, *114* (10), 4340−4344.

https://doi.org/10.1021/acsomega.4c03606
ACS Omega 2024, 9, 31925−31932